Research Article

A Modified Model for Kinetic Analysis of Petroleum Coke

Iman Eslami Afrooz [ID] **and Dennis Ling Chuan Ching**

Department of Fundamental and Applied Sciences, Universiti Teknologi PETRONAS, Seri Iskandar 32610, Malaysia

Correspondence should be addressed to Iman Eslami Afrooz; imaneslami@hotmail.com

In this study, a nonisothermal kinetics analysis of petcoke was performed at heating rates of 10, 15, and 20°C/min using thermal gravimetric analysis (TGA). The behaviour of petcoke at different gasification stages (dewatering, volatilization, char burning, and burnout) was studied. The effect of heating rate on the activation energy of petcoke gasification was also investigated. The activation energy of petcoke was estimated using different kinetic models that include volume reaction model (VRM), shrinking core model (SCM), random pore model (RPM), Coats and Redfern model (CRM), and normal distribution function (NDF). The NDF model was modified in this study. It was found that the experimental data were best fitted with the modified normal distribution function (MNDF) and SCM. The results also showed that activation energy decreases as heating rate increases, leading to reduction in gasification completion time.

1. Introduction

Petcoke is a heavy crude oil refining coproduct. It is identified as a black-colored, carbon-rich solid. Despite the few human health or environmental risks posed by the exploitation of petcoke, it has a high economic value and many industrial applications. It is mostly used as a boiling and combusting fuel in industrial, power generation, and cement plants. Moreover, it can be used as a raw material in manufacturing processes. In addition, petcoke is a promising substitute for steam coal in power plants because of its higher heating value, carbon content, and low ash, compared to bituminous coals [1, 2]. However, petcoke gasification is a difficult process because of its high content of fixed carbon [3, 4] and low volatile matter [5]. Moreover, the mass transfer of petcoke is influenced by the porosity, pore size, and volume as well as diffusivity and tortuosity of the carbon substrate [6, 7]. To tackle this issue, different solutions have been studied such as modifying particle size, inclusion of catalysts, and cogasification [2, 8]. In cogasification, as an example, petcoke is combined with additional fuels such as coal or biomass to improve its low reactivity [9, 10]. Appropriate catalysts can also be incorporated into the gasification of petcoke to improve their low reactivity [4, 11, 12].

The other alternative approach to achieve the high carbon conversion is to increase the residence time of the fuel particles [7].

The above discussion demonstrates the importance of petcoke gasification development. Therefore, understanding the gasification kinetics of fuels is key to finding solutions to potential problems of gasification as well as improving operating conditions to develop efficient gasification processes. In addition, a detailed understanding of reaction kinetics is vital for the feasibility, design, and scaling of gasification applications. It will also provide valuable information for proper design and operation of gasifiers. Therefore, the combustion characteristics, chemical elements, and technical analysis of the fuels fed into the gasification reactor must be understood. For this purpose, thermal gravimetric analysis (TGA) and derivative thermogravimetry (DTG) curves provide information on fuel reactivity properties such as ignition, peak, and burnout temperatures [13, 14]. The change in the mass of the sample caused by devotilization during thermal decomposition is monitored by TGA as a function of temperature or time. The maximum reaction rate of the sample can then be obtained through the first derivative of the TGA curve (dx/dt). This curve is known as DTG.

In 1975, Tyler and Smith [15] studied the reactivity of petcoke with CO_2 over a temperature range of 1018–1178 K. A rate order of approximately 0.6 and activation energies in the range of 203–237 kJ/mol were obtained for the petcoke with respect to carbon dioxide concentration. A constant rate order and activation energy of about 45% with a burn-off range of 21%–45% were reported. Revankar et al. [16] investigated the effect of particle size, porosity, and thickness on the steam gasification of petcoke, where they reported increase in the rate constant with decrease in both grain size and pellet size, with or without a catalyst. In contrast, activation energy was found to be independent of particle size for the noncatalytic gasification, but the frequency factor decreased with particle size. However, this trend is in reverse for catalytic gasification.

Zou et al. [17] investigated the kinetic characteristics of petcoke gasification with CO_2 at 1248–1323 K and 0.1 MPa. They proposed a normal distribution function model (NDF) to fit the kinetics data. The gasification rate was observed to increase with the conversion rate (X) up to the peak of $X = 0.3$. The activation energy and reaction order range of 198 kJ/mol and 0.54–0.88 were reported, respectively, for the CO_2 gasification of petcoke. Yoon et al. [18] conducted a TGA study of coal and petroleum coke for cogasification at 15°C/min heating rate. The petcoke activation energies of 53.73 and 46.03 kJ/mol were reported using kinetic models of the shrinking core model (SCM) and the integrated model or the modified volume reaction model (MVRM), respectively. In a similar study, Nemanova et al. [19] explored the cogasification of petcoke and biomass at a rate of 10°C/min using TGA. They analyzed TGA data using the volume reaction model (VRM) and determined an activation energy value of 121.5 kJ/mol for the petcoke steam gasification. Recently, Jayaraman and Gokalp [8] studied the effect of particle size on steam gasification of petcoke using TGA and mass spectrometry analysis. Relatively high reaction rates and 90% conversion efficiency were observed for smaller-sized particles (30 μm). The study proposed an operation temperature of ≥950°C for petcoke gasification under steam or blended steam ambiences with efficient fuel conversion.

A summary of the studies discussed above is given in Table 1. Without doubt, the review shows there is no discrete activated state as confirmed by the wide variations of calculated activation energies [20]. However, the existing models have some limitations. For example, the assumptions of the SCM model may not accurately match the real conditions, even though the model is considered the most appropriate simple representation for the majority of reacting gas-solid systems [21]. According to SCM, the reaction occurs first at the ash layer and the outer skin of the particle and then moves into the nonreacted core. Alternatively, the reaction may occur along a diffuse front, which is a kind of intermediate behaviour between the SCM and CRM models. In addition, considering the fast reactions, the heat release rate is sufficiently high to cause significant temperature gradients within the core of the particle. However, there is a lack of kinetic models that accurately analyze the reactions of more complex heat distributions in gas-solid systems. Therefore, this study investigates the gasification characteristics and kinetic analysis of petcoke using TGA and proposed modified normal distribution function (MNDF) at differential heating rates. Based on the kinetic data collected by TGA, some of the common kinetic models were utilized to estimate the activation energy of petcoke. The results were then comparatively analyzed and discussed.

2. Materials and Methods

2.1. Sample Preparation.
For this study, petcoke obtained from PETRONAS Melaka Refinery with a Hardgrove Grindability Index (HGI) of 111 and a particle size range of 5–20 mm was used. The petcoke was crushed and milled to a size of 0.7 mm. It was then dried for 24 hours at 110°C using an industrial oven. Afterward, the combustion characteristics of petcoke were investigated using PerkinElmer STA 6000. The initial weights of the petcoke samples were varied since the TGA results were unaffected by the sample weight. To investigate the effect of heating rate on the gasification phases, TGA experiments were carried out at heating rates of 10, 15, and 20°C/min. In addition, an untreated petcoke sample (as received) was used to investigate the influence of sample preparation conditions on TGA curves. The descriptions of samples used in this study are outlined in Table 2.

2.2. Ultimate and Proximate Analysis.
Ultimate analysis was carried out to determine the percentage of carbon, hydrogen, nitrogen, and sulphur chloride of the petcoke using a CHNOS elemental analyzer under consideration of ASTM D5373. Proximate analysis was carried out using ASTM D5142-90 to acquire preliminary results on the moisture content, volatile matter, fixed carbon, and ash content of petcoke samples. In addition, a bomb calorimeter with standard reference of the ASTM D5865 test method was used to determine the calorific value of the samples. Dried petcoke sample was used for both ultimate and proximate analysis. However, the calorific value test was carried out on both dried and untreated petcoke samples.

Table 3 shows the results for ultimate, proximate, and calorific value analyses. Different heating rates of 10, 15, and 20°C/min were used, while the TGA experiment temperature was kept at 800°C. The nitrogen and oxygen flow rates were kept at 100 ml/min for all experiments. The change in sample weight was recorded every second. A continuous supply of nitrogen was maintained for 40 minutes to eliminate moisture until the reaction temperature specified for the generation of char was attained. Afterward, the effect of heating rate on the ignition temperature and ignition time of petcoke was analyzed by burning each petcoke sample under different heating rates in the presence of oxygen. Finally, the combustion characteristics of the char were measured for each sample.

2.3. Kinetic Analysis.
Similar to other organic or chemical matters like biomass or coal, the kinetic of petcoke decomposition can also be predicted by the following equation:

TABLE 1: Summary of kinetic models.

Reference	Particle size (mm)	Carbon and ash content (%)	Gasification medium/pressure (kPa)	Heating rate (°C/min)	TGA maximum temperature (°C)	Kinetic model	Activation energy (kJ/mol)
[15]	2.9, 0.9 0.22	96.4, 96.8, 96.9 0.75, 0.40, 0.43	CO_2/26 and 118	10	745–905	—	203–237
[16]	0.037–0.59	99 0.3	Steam/atm	20–400 25–880	695–880	SCM	26–30.6 34*–52*
[17]	9.963	90.25 0.56	CO_2/100	25	975–1050	NDF	198
[18]	0.02–0.05	87.16 0.25	Air/atm	15	1100, 1200 1300, 1400	SCM MVRM	53.73 46.03
[19]	1–1.5	92.3 1.4	Steam/atm	10	1250	VRM	121.5

*With catalyst.

TABLE 2: Samples descriptions.

Samples	Initial weight (mg)	Preparation conditions	Heating rate (°C/min)	TGA temperature (°C)
1	7.684	Dried for 24 h	10	800
2	8.964	Dried for 24 h	15	800
3	9.963	Dried for 24 h	20	800
4	7.443	As received	15	800

TABLE 3: Ultimate, proximate, and calorific value analysis of petcoke.

Test	Parameter	Result
Ultimate analysis (wt.%)	Carbon	83.29
	Hydrogen	3.576
	Nitrogen	1.68
	Sulphur	5.528
Proximate analysis (wt.%)	Moisture	6.0
	Volatile matter	14.8
	Ash	0.14
	Fixed carbon	79.06
Calorific value (J/g)	Dried sample	35875
	As received	36211

$$\frac{dX}{dt} = Kf(X), \tag{1}$$

where dX/dt, K, $f(X)$, and X are the isothermal reaction rate, the reaction rate constant, the reaction model equation, and the extent of reaction (or the conversion rate), respectively.

The reaction rate K is presented by the Arrhenius expression as follows:

$$K = A \exp\left(-\frac{E_a}{RT}\right). \tag{2}$$

By substituting equation (2) into equation (1), the rate law can be expressed as

$$\frac{dX}{dt} = Kf(X) = A \exp\left(-\frac{E_a}{RT}\right) f(X). \tag{3}$$

The extent of reaction, X, can be obtained using the following expression:

$$X = \frac{m_0 - m_t}{m_0 - m_f}, \tag{4}$$

where m_0, m_t, and m_f are the initial sample mass, sample mass at time t, and final sample mass, respectively.

Some of the important rate models, $f(X)$, used to describe the kinetic behaviour of solid-state reactions were listed in ref. [22]. Among them, the VRM [23], SCM [21], random pore model (RPM) [24], MVRM [25, 26], NDF [17], and Coats and Redfern (CR) model [27, 28] have been used by researchers to predict the kinetic parameters of petcoke. Based on the VRM (or homogeneous model) assumption, the particle density changes uniformly due to the distribution of gas inside the solid particles. According to the VRM, the reaction kinetic expression can be described as

$$\frac{dX}{dt} = K_v (1 - X), \tag{5}$$

where $(1 - X)$ is the remaining fraction of volatile material in the sample.

The SCM was first established by Yagi and Kunii [29]. SCM assumes that the reaction first occurs at the outer skin of the spherical particle, and it then moves into the non-reacted core which shrinks in size gradually during reaction process. According to SCM, the reaction kinetic model is as follows:

$$\frac{dX}{dt} = K_s (1 - X)^{2/3}. \tag{6}$$

The RPM takes into account the pore structure and its evolution in the course of reaction. Based on the RPM, the gasification rate can be written as

$$\frac{dX}{dt} = K_r (1 - X)(1 - \psi \ln(1 - X))^{1/2}, \tag{7}$$

where ψ is the particle structure parameter. The RP model with the value of ψ equal to zero gives the VR model.

The volume reaction model was improved to MVRM (or integrated model) by Kasaoka et al. [25] and Yang et al. [26]. It was extended for all reaction orders by adding a new parameter (n) as follows:

$$\frac{dX}{dt} = K_m (1 - X)^n. \tag{8}$$

Zou et al. [17] proposed the normal distribution function (NDF) as a model to predict kinetic parameters. The conventional distribution function is approximated by a Gaussian distribution that yields a mean value and standard deviation. Based on NDF, the reaction kinetic model can be written as

$$\frac{dX}{dT} = K_d \exp\left(-\frac{(X - X_m)^2}{2\omega^2}\right), \tag{9}$$

where X_m and ω are the maximal gasification rate and the width of the curve, respectively.

On the contrary, the reaction rate can be presented as a function of temperature for nonisothermal solid-state reactions:

$$\frac{dX}{dt} = \frac{dT}{dt}\frac{dX}{dT} = \beta\frac{dX}{dT}, \tag{10}$$

where β is the heating rate and dX/dT is the nonisothermal reaction rate.

Considering equations (3) and (10), the reaction rate can be represented as

$$\frac{dX}{dt} = \beta\frac{dX}{dT} = A \exp\left(-\frac{E_a}{RT}\right) f(X). \tag{11}$$

By taking natural logarithms of each side,

$$\ln\left(\frac{dX}{dt}\right) = \ln\left(\beta\frac{dX}{dT}\right) = \ln[Af(X)] - \frac{E_a}{RT}. \tag{12}$$

Integration of equation (11) yields

$$g(X) = \int_0^X \frac{dX}{f(X)} = \frac{A}{\beta}\int_0^T \exp\left(-\frac{E_a}{RT}\right) dT. \tag{13}$$

Equation (13) is the integral expression of the rate law. If we consider (E_a/RT) as u, equation (13) becomes

$$g(X) = \frac{AE_a}{\beta R}\int_X^\infty \frac{\exp^{-u}}{u^2} = \frac{AE_a}{\beta R} p(u). \tag{14}$$

The $p(u)$ in equation (14) known as the temperature integral cannot be integrated by one of the methods of calculus. However, this is not a serious limitation because it can be approximated via empirical interpolation formulas like an integral method based on the Coats and Redfern (CR) equation [27, 28]. Therefore, $p(u)$ in equation (14) can be estimated using a Taylor series expansion to yield the following expression [22]:

$$g \ln\left(\frac{-\ln(1 - X)}{T^2}\right) = \ln\left[\frac{AR}{\beta E_a}\left(1 - \frac{2RT}{E_a}\right)\right] - \frac{E_a}{RT}. \tag{15}$$

To begin, we studied the weight reduction of petcoke for different heating rates. Afterward, some of the abovementioned models were used to fit the experimental data obtained by TGA. A modified form of NDF was then proposed. Finally, using an Arrhenius plot, the accuracy of the kinetic models in petcoke activation energy approximation was comparatively evaluated.

3. Results and Discussion

3.1. TGA and DTG Analysis. Petcoke was evaluated using TGA analysis to understand its ignition temperature and combustion characteristics. The weight reduction for different heating rates of 10, 15, and 20°C/min is demonstrated in Figure 1. Since there was no evidence of weight loss within the first 30 minutes of the TGA, Figures 1(a) and 1(b) only depict the values that exceed 240°C and 30 min, respectively. It is discernible from the TGA that the dewatering stage starts around 243°C (at 32.13 min), 463°C (at 39.40 min), 419°C (at 30.00 min), and 465°C (at 39.51 min) and continues till the temperature reached approximately 518°C (at 57.71 min), 523°C (at 42.08 min), 525°C (at 34.25 min), and 519°C (at 41.98 min) for samples 1 to 4, respectively. Taking into cognizance the dewatering stage, the weight of all samples reduced by nearly 6%. However, the differential weight values can be attributed to the different applied heating rates.

It is also important to note that the time required for complete petcoke dewatering for treated and untreated samples (samples 2 and 4) is almost the same. Therefore, since the effect of sample drying is negligible, more energy can be saved by using untreated samples. Volatilization is initiated immediately after the dewatering stage for all samples and is completed at about 542°C (at 58.38 min), 548°C (at 42.65 min), 554°C (at 34.85 min), and 542°C (at 42.45 min) for samples 1 to 4, respectively. Subsequent to the volatilization stage is the char combustion phase. The combustion process was finally completed at different temperatures of 572°C (at 61.16 min), 595°C (at 45.78 min), 620°C (at 38.21 min), and 583°C (at 44.83 min) for samples 1 to 4, respectively. The gray area in Figure 1(b) shows our implementations for petcoke combustion, which can be used as a tool to predict the petcoke combustion behaviour under certain heating rates. This specifically implies the rate of petcoke weight loss during the combustion reaction at heating rates between 10 and 20°C/min can be predicted from the gray area.

To study the effect of reaction rate on different reaction stages, the start and end points of time and temperature for each phase were calculated and the results are presented in Table 4. Irrespective of the heating rates employed, the time required for total volatilization was the same. A similar trend can be observed for the combustion stage. However, there is a slight disparity between the temperature values of the volatilization and combustion stages, which can be attributed to the different heating rates applied. This indicates that the effect of heating rate on the volatilization and combustion stages is negligible. Significant deviations are only observed for the time required for the dewatering stage to be completed. Therefore, the most pertinent deduction is that the time required for moisture removal from petcoke can be
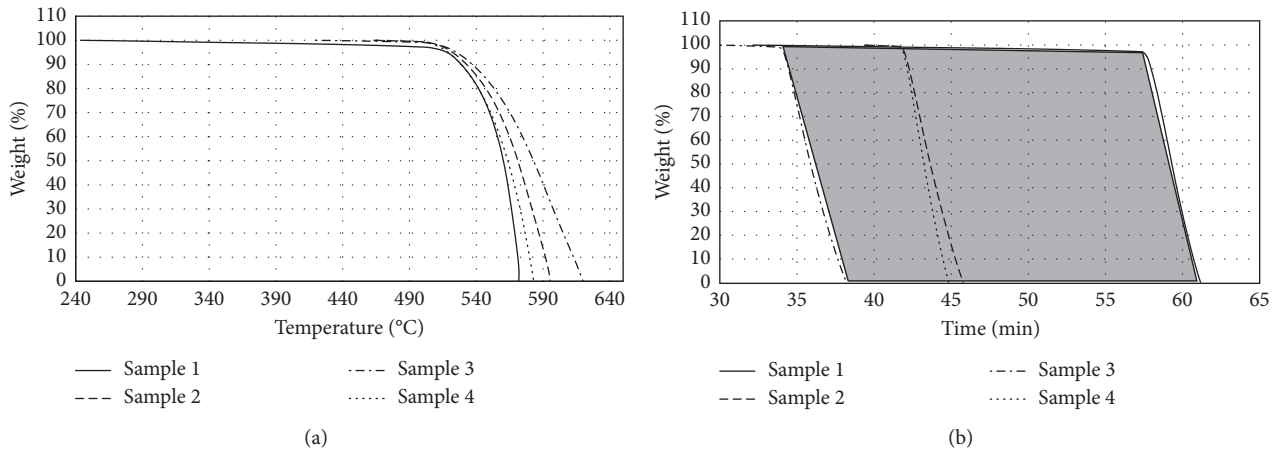
FIGURE 1: Rate of petcoke weight loss (%) vs. (a) temperature (°C) and (b) time (min) for different samples. The gray area shows the range in which our implementations for petcoke combustion were applied.

TABLE 4: Reaction stages characterization.

| Sample | Heating rate (°C/min) | Reaction stage | | | | | |
| | | Dewatering | | Volatilization | | Combustion | |
		Time (min)	Temp (°C)	Time (min)	Temp (°C)	Time (min)	Temp (°C)
1	10	25.58	275	0.67	24	2.78	30
2	15	2.68	60	0.57	25	3.13	47
3	20	4.25	106	0.6	29	3.36	66

significantly reduced by increasing the heating rate. Moreover, comparison of the heating rates shows 15°C/min is the most effective for all stages of petcoke gasification.

The TGA and DTG curves for the thermal decomposition of petcoke at a heating rate of 15°C/min are shown in Figure 2(a). As earlier explained, the TGA contrasts the weight loss of the petcoke with temperature change, whereas the DTG represents the time derivative of the weight loss for the same temperature change as TGA. It can be inferred from Figure 2(a) that the rate of weight loss is maximum at 558°C (peak temperature). Cursory evaluation of the TGA curve indicates the peak temperature occurred in the char combustion phase. Thus, the rapid weight reduction corresponds to the combustion phase.

It is also important to mention that the change in the values of derivative weight, as observed from the DTG curve, indicates that the progressive thermal breakdown of the organic matter present in the petcoke occurs within the range of 480–620°C. In addition, the burnout temperature of 620°C represents the temperature where sample oxidation is complete. The derivative weight curves for the thermal decomposition of petcoke at different heating rates are shown in Figure 2(b). It is observed that the maximum weight losses for heating rates between 10 and 15°C/min occur at almost the same temperature of 558°C. Moreover, the maximum weight loss for the treated sample (sample 1) and the untreated sample (sample 2) occurred at 558 and 556°C, respectively. However, at the higher heating rate of 20°C/min, the maximum weight loss was recorded at 568°C.

Conversely, the DTG profiles clearly show that the rate of weight loss slightly decreases with the increase in heating rate. The maximum conversion rates of −32.15, −29.87, and −28.52% min^{-1} were observed for the heating rates of 10, 15, and 20°C/min, respectively. Remarkably, the DTG profile of the untreated sample (sample 4) shows a higher rate of weight loss (−37.47% min^{-1}) than the others. It is evident that the reaction sensitivity of petcoke to heating rate and sample treatment is very low.

3.2. Arrhenius Plot and Activation Energy. The reaction rates, K, were calculated using selected kinetic models that include, VRM, SCM, RPM, NDF, and CRM. The Arrhenius plots for the gasification reaction of petcoke (Figure 3) were derived using the logarithmic reaction rate $\ln(K) \min^{-1}$ versus the reciprocal gasification temperature $1000/T\,K^{-1}$. It is discernible from the Arrhenius plots that the logarithmic gasification reaction rate exhibits a linear relationship with temperature for almost all kinetic models and reaction rates, with the exception of 10°C/min. As observed in Figure 3, the slope of $\ln(K)$ versus $1000/T$ becomes steeper as the heating rate declines. Given the proportionality of the activation energy (E_a) with the slope of the Arrhenius plot, it can be inferred that the activation energy increases as heating rate decreases.

The activation energies E_a for different kinetic models were determined using equation (16), and results are presented in Table 5 for comparison.
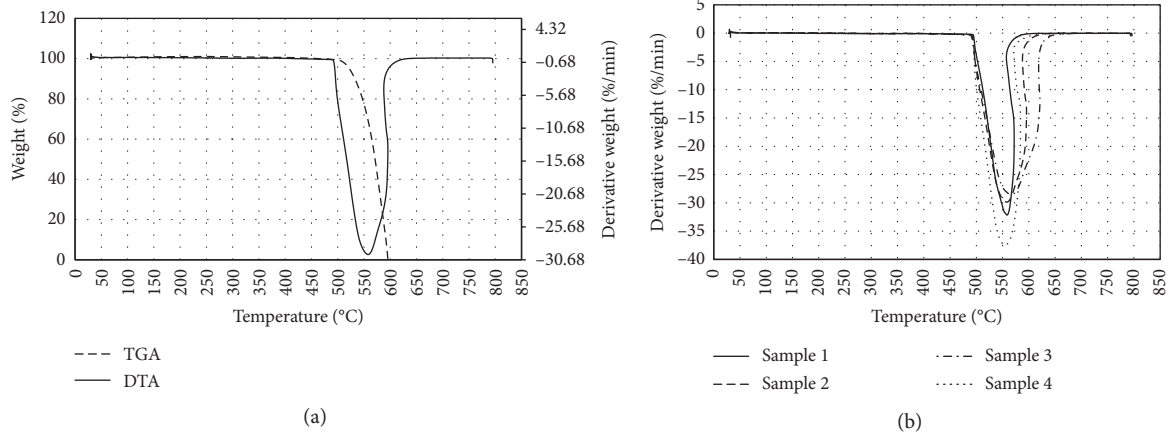
Figure 2: Plots of (a) TGA and DTG curves and (b) DTG curves for different heating rates.
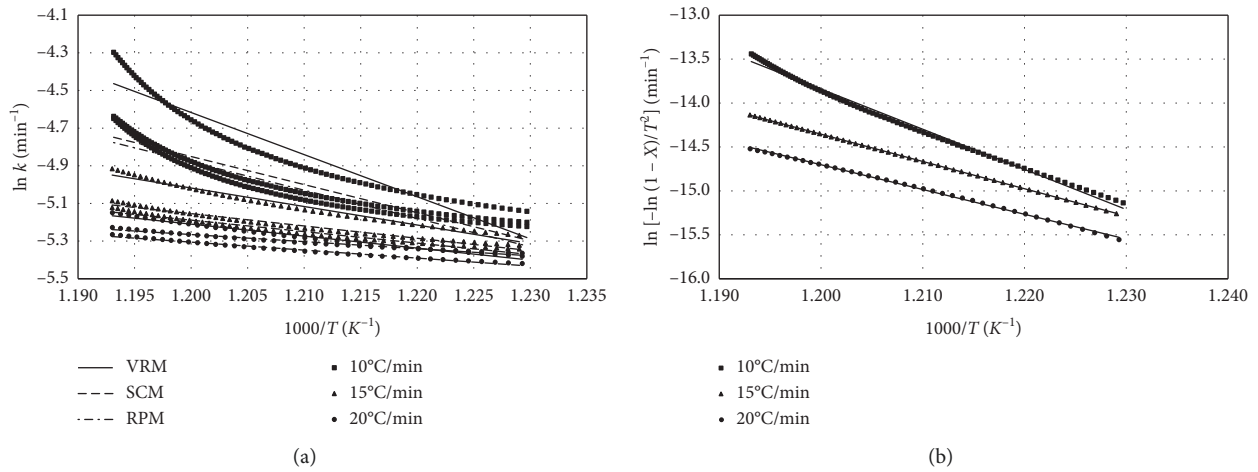

Figure 3: Comparison of Arrhenius plots for different heating rates of 10, 15, and 20°C/min vs. (a) VR, SC, and RP models; (b) CR model.

Table 5: Activation energy of petcoke.

Heating rate (°C/min)	Activation energy (kJ/mol)					
	VRM	SCM	RPM	CRM	NDF	MNDF
10	186	124	124.8	379.9	635.7	124
15	81.7	54.5	50.7	258.1	411.3	80.2
20	53	35.3	31.3	234.5	320.2	62.5

$$\text{slope} = -\frac{E_a}{R}, \tag{16}$$

where slope is the slope of $\ln(K)$ versus $1/T$ from the Arrhenius plot.

Based on the data outlined in Table 5, there is a significant difference between the activation energy values obtained by CRM and NDF and those acquired by the other kinetic models. This difference can be attributed to systematic errors associated with the calculation of E_a using the integral isoconversional kinetic models. Considering each kinetic model, it can be noted that activation energies obtained from different heating rates were not the same and they all increase with decreased heating rates. This is because more energy is required to initiate release of the refractory

molecules enclosed in petcoke in the form of volatiles when using lower heating rates. The comparative analysis of E_a values obtained in this study with those reported in earlier studies (Table 1) shows that more reliable E_a values can be estimated using SCM, RPM, and VRM, while those obtained using NDF and CRM are overestimated. The results indicated that increasing the heating rate leads to reduction in activation energy. As a result, less energy is needed to activate atoms or molecules to a state where they can undergo a chemical reaction. For example, using SCM, the activation energy of petcoke is reduced by 71.53% with the increase in heating rate from 10 to 20°C/min.

3.3. Modified Normal Distribution Function (MNDF).
As stated above, the NDF overestimated the values of activation energy. Nonetheless, NDF has some features which make it a valuable approximation function for complex distributions of variables. The NDF model was then modified by calculating the right values of maximal gasification rate (X_m) and the curve width (ω) of the normal distributed function. Considering the normal distribution function (equation (9)), its exponential function increases to zero while the value of ω
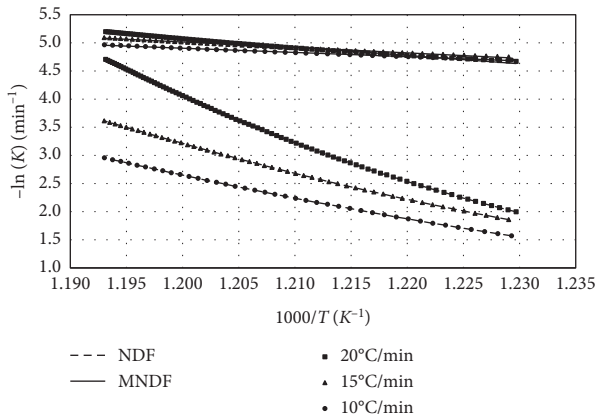
Figure 4: Comparison of Arrhenius plots for MNDF and NDF.

decreases. Meanwhile, the value of conversion (X) changes from 0 to 1. Consequently, the graph of NDF for X_m equal to mean is symmetric with respect to the line X equal to mean ($X = $ mean). Considering these features of NDF, choosing the right values of ω and X_m is necessary to best fit the graph of experimental data with the straight line. To this end, the values of 1 and 0.736 are proposed in this study for X_m and ω, respectively. Using these values, the following modified NDF (MNDF) is proposed:

$$\frac{dX}{dt} = K_d \exp\left[-\frac{(X-1)^2}{1.0834}\right]. \qquad (17)$$

Plots of $-\ln(k)$ versus $1000/T$, derived from different heating rates and MNDF and NDF kinetic models, are illustrated in Figure 4.

It is worthwhile to mention that using NDF, the logarithmic reaction rate results in a straight line with positive slope. Therefore, the negative logarithmic function ($-\ln$) was used in this study to make the slope of the Arrhenius graph negative. This change in sign does not affect the results of activation energy. However, this finding was not reported in the literature [17]. It can be clearly seen in Figure 4 that the MNDF yields much tighter curves that establish a better fit with experimental data than the conventional NDF model. Furthermore, compared with the NDF model, the MNDF provided a better minimization of the discrepancy in calculated activation energies. The activation energies are consistent with those extracted from the literature.

4. Conclusions

In this study, TGA was performed on petcoke to study its combustion characteristics under different heating rates. The different stages of combustion, namely, dewatering, volatilization, char burning, and burnout for petcoke were examined. Some common kinetic models (VRM, SCM, RPM, CRM, and NDF) were utilized to estimate the activation energy of the combustion of petcoke. The NDF model was modified to best fit the experimental data. The kinetic analysis showed that the combustion results of petcoke under the heating rate of 10°C/min show a longer transition stage between dewatering and volatilization. It was also

found that the activation energy of petcoke is significantly affected by increase in heating rate. The TGA results revealed that the total time needed for gasification of petcoke was shortened with the use of 20°C/min heating rate, which indicated that increasing the heating rate leads to reduction in activation energy. Thus, shorter gasification finishing time is expected while using higher heating rate. The proposed modified kinetic model (MNDF) was found to accurately predict the gasification kinetics the most and achieved 50% reduction in activation energy. In addition, the results show that the duration for complete petcoke combustion can vary from 38 to 61 minutes. The proposed kinetic model provides valuable information for proper design and operation of the gasifier reactors. It also improves the understanding and development of the gasification process.

Data Availability

The TGA data used to support the findings of this study are available from the corresponding author upon request.

Conflicts of Interest

The authors declare that there are no conflicts of interest regarding the publication of this paper.

Acknowledgments

References

[1] E. Furimsky, "Gasification of oil sand coke: review," *Fuel Processing Technology*, vol. 56, no. 3, pp. 263–290, 1998.

[2] B. N. Murthy, A. N. Sawarkar, N. A. Deshmukh, T. Mathew, and J. B. Joshi, "Petroleum coke gasification: a review," *The Canadian Journal of Chemical Engineering*, vol. 92, no. 3, pp. 441–468, 2014.

[3] X. Zhan, J. Jia, Z. Zhou, and F. Wang, "Influence of blending methods on the co-gasification reactivity of petroleum coke and lignite," *Energy Conversion and Management*, vol. 52, no. 4, pp. 1810–1814, 2011.

[4] X. Zhan, Z. Zhou, and F. Wang, "Catalytic effect of black liquor on the gasification reactivity of petroleum coke," *Applied Energy*, vol. 87, no. 5, pp. 1710–1715, 2010.

[5] J. Chen and X. Lu, "Progress of petroleum coke combusting in circulating fluidized bed boilers—a review and future perspectives," *Resources, Conservation and Recycling*, vol. 49, no. 3, pp. 203–216, 2007.

[6] E. Furimsky, "Gasification reactivities of cokes derived from athabasca bitumen," *Fuel Processing Technology*, vol. 11, no. 2, pp. 167–182, 1985.

[7] C. Higman and M. van der Burgt, *Gasification*, Gulf Professional Publications, Amsterdam, Netherlands, 2nd edition, 2008.

[8] K. Jayaraman and I. Gokalp, "Gasification characteristics of petcoke and coal blended petcoke using thermogravimetry and mass spectrometry analysis," *Applied Thermal Engineering*, vol. 80, pp. 10–19, 2015.

[9] J. Fermoso, B. Arias, M. G. Plaza et al., "High-pressure co-gasification of coal with biomass and petroleum coke," *Fuel Processing Technology*, vol. 90, no. 7-8, pp. 926–932, 2009.

[10] J. Fermoso, B. Arias, B. Moghtaderi et al., "Effect of co-gasification of biomass and petroleum coke with coal on the production of gases," *Greenhouse Gases: Science and Technology*, vol. 2, no. 4, pp. 304–313, 2012.

[11] Z.-J. Zhou, Q.-J. Hu, X. Liu, G.-S. Yu, and F.-C. Wang, "Effect of iron species and calcium hydroxide on high-sulfur petroleum coke CO_2 gasification," *Energy & Fuels*, vol. 26, no. 3, pp. 1489–1495, 2012.

[12] S. H. Lee, S. J. Yoon, H. W. Ra, Y. I. Son, J. C. Hong, and J. G. Lee, "Gasification characteristics of coke and mixture with coal in an entrained-flow gasifier," *Energy*, vol. 35, no. 8, pp. 3239–3244, 2010.

[13] C. Wang, F. Wang, Q. Yang, and R. Liang, "Thermogravimetric studies of the behavior of wheat straw with added coal during combustion," *Biomass and Bioenergy*, vol. 33, no. 1, pp. 50–56, 2009.

[14] F. Trejo, M. S. Rana, and J. Ancheyta, "Thermogravimetric determination of coke from asphaltenes, resins and sediments and coking kinetics of heavy crude asphaltenes," *Catalysis Today*, vol. 150, no. 3-4, pp. 272–278, 2010.

[15] R. J. Tyler and I. W. Smith, "Reactivity of petroleum coke to carbon dioxide between 1030 and 1180 k," *Fuel*, vol. 54, no. 2, pp. 99–104, 1975.

[16] V. V. S. Revankar, A. N. Gokarn, and L. K. Doraiswamy, "Studies in catalytic steam gasification of petroleum coke with special reference to the effect of particle size," *Industrial & Engineering Chemistry Research*, vol. 26, no. 5, pp. 1018–1025, 1987.

[17] J. H. Zou, Z. J. Zhou, F. C. Wang et al., "Modeling reaction kinetics of petroleum coke gasification with CO_2," *Chemical Engineering and Processing: Process Intensification*, vol. 46, no. 7, pp. 630–636, 2007.

[18] S. J. Yoon, Y.-C. Choi, S.-H. Lee, and J.-G. Lee, "Thermogravimetric study of coal and petroleum coke for co-gasification," *Korean Journal of Chemical Engineering*, vol. 24, no. 3, pp. 512–517, 2007.

[19] V. Nemanova, A. Abedini, T. Liliedahl, and K. Engvall, "Co-gasification of petroleum coke and biomass," *Fuel*, vol. 117, pp. 870–875, 2014.

[20] P. D. Garn, "Kinetic parameters," *Journal of Thermal Analysis and Calorimetry*, vol. 13, no. 3, pp. 581–593, 1978.

[21] C. N. Satterfield, "Chemical reaction engineering, Octave Levenspiel, Wiley, New York (1972). 578 pages. $16.95," *AIChE Journal*, vol. 19, no. 1, pp. 206-207, 1973.

[22] J. E. White, W. J. Catallo, and B. L. Legendre, "Biomass pyrolysis kinetics: a comparative critical review with relevant agricultural residue case studies," *Journal of Analytical and Applied Pyrolysis*, vol. 91, no. 1, pp. 1–33, 2011.

[23] M. Ishida and C. Y. Wen, "Comparison of zone-reaction model and unreacted-core shrinking model in solid—gas reactions—I isothermal analysis," *Chemical Engineering Science*, vol. 26, no. 7, pp. 1031–1041, 1971.

[24] S. K. Bhatia and D. D. Perlmutter, "A random pore model for fluid-solid reactions: I. Isothermal, kinetic control," *AIChE Journal*, vol. 26, no. 3, pp. 379–386, 1980.

[25] S. Kasaoka, Y. Sakata, and C. Tong, "Kinetic evaluation of reactivity in carbon dioxide-gasification of various coal chars, and comparison with steam-gasification," *Journal of the Fuel Society of Japan*, vol. 62, no. 5, pp. 335–348, 1983.

[26] X. F. Yang, J. Zhou, X. Gong, and Z. Yu, "Kinetic and characteristic study of char-H_2O gasification by isothermal thermogravimetry," *Coal Conversion*, vol. 2003, no. 4, pp. 46–50, 2003.

[27] A. W. Coats and J. P. Redfern, "Kinetic parameters from thermogravimetric data," *Nature*, vol. 201, no. 4914, pp. 68-69, 1964.

[28] A. W. Coats and J. P. Redfern, "Kinetic parameters from thermogravimetric data. II," *Journal of Polymer Science Part B: Polymer Letters*, vol. 3, no. 11, pp. 917–920, 1965.

[29] S. Yagi and D. Kunii, "Studies on combustion of carbon particles in flames and fluidized beds," *Symposium (International) on Combustion*, vol. 5, no. 1, pp. 231–244, 1955.